ATLAS measurements of CP Violation and Rare decays processes with Beauty mesons

Oleg Meshkov (MSU & Lebedev PI)

10th International Workshop on Charm Physics (Charm 2020)

On behalf of the ATLAS Collaboration

B-physics at ATLAS

- ATLAS Run 2: 139 fb^{-1} of pp collisions at $\sqrt{s}$ = 13 TeV collected in 2015-2018
- Producing ~2.5 million $b\bar{b}$ pairs/second, B_s , B_c , Λ_b, etc. available
- Program focused mostly on muonic final states, fully reconstructable
- Typical trigger: low-p_T di-muons at low invariant mass, using information from inner tracker(pT > 0.4 GeV, $|\eta| < 2.5$) and muon detectors(triggering ($|\eta| < 2.4$), precision tracking ($|\eta| < 2.7$)).
- In Run2: Insertable B-Layer (IBL) resolution in b-hadron proper decay time was ~70 fs
- B-physics trigger rate up to ~ 200 Hz

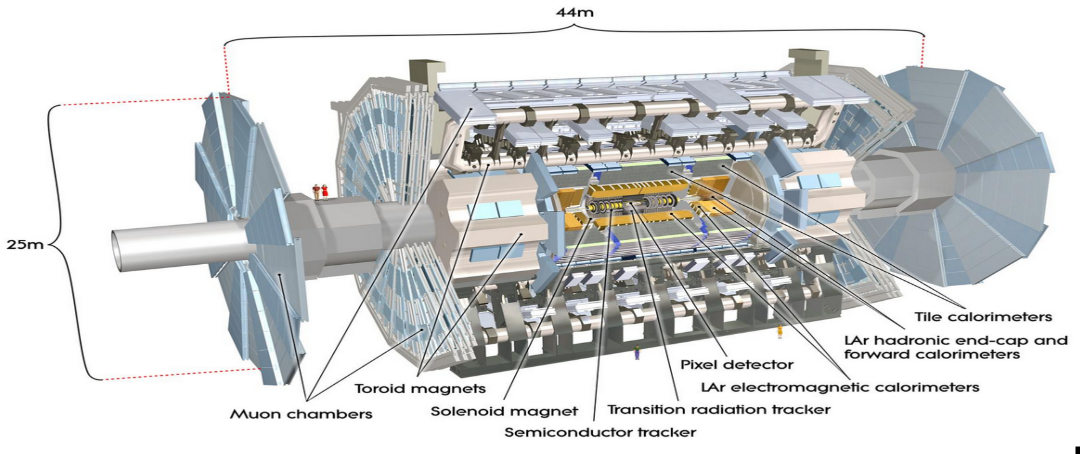

ATLAS Run-1 analysis:
CP-violation: JHEP 08 (2016) 147
Rare decays: Eur. Phys. J. C 76 (2016) 513

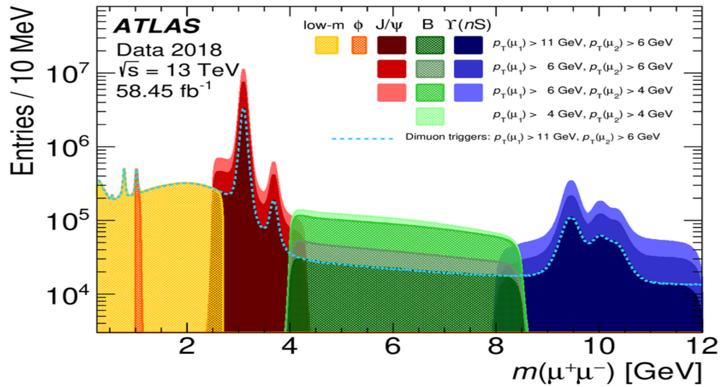

Latest results on rare decays and CP-violation

- Measurement of CP-violating phase φ_s (and other parameters) in the $B_s \rightarrow J/\psi\phi$ decay using 2015-2017 data (80.5 fb^{-1})
  - Eur. Phys. J. C 81 (2021) 342
- Measurement of the branching ratio of $B_s \rightarrow \mu\mu$ decays using 2015-2016 data (26.3 fb^{-1}), combination with CMS and LHCb (ATLAS-CONF-2020-049)
  - JHEP 04 (2019) 098

Measurement of the CP-violating phase ϕ_s in $B_s \to J/\psi\phi$ decays in ATLAS at 13 TeV

CP violation in $B_s \to J/\psi\phi$

- Interference of direct decay and decay with mixing into the same final state of $B_s \to J/\psi\phi$ decay gives rise to time-dependent CP violation (CPV)

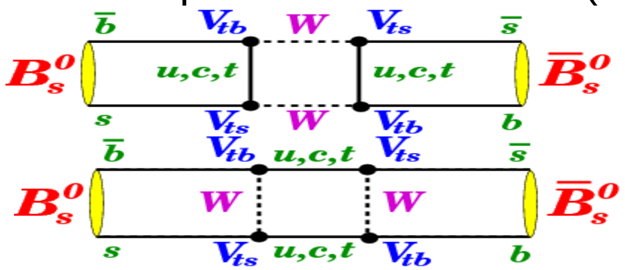

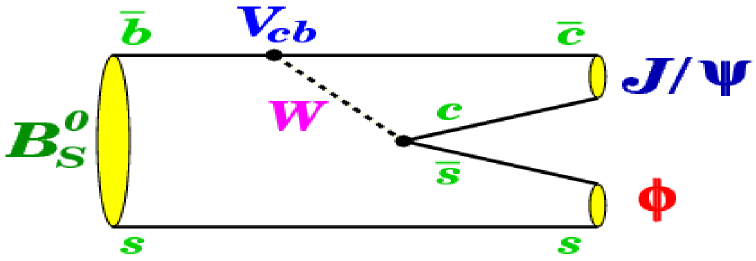

- CPV phase φ_s is weak phase difference between the B_s - $\bar{B}_s$ mixing amplitude and the $b \to c\bar{c}s$ decay amplitude
- In the SM the phase φ_s is small and is related to CKM quark matrix:

$$\varphi_s \equiv -2\beta_s = -2\arg\left(\frac{-V_{ts}V^*_{tb}}{V_{cs}V^*_{cb}}\right) = -0.03696^{+0.00072}_{-0.00082}\, rad$$

Phys. Rev. D 91 (2015) 073007

- New Physics (NP) processes could contribute to the mixing box diagrams, potentially allowing for large deviations in φ_s from the SM prediction
- Alongside φ_s, other quantities are describing the differential decay rate:
  - Decay widths of the two mass eigenstates
  - CP even/odd state amplitudes and phases

Data Analysis

Eur. Phys. J. C 81 (2021) 342

Data:

- Using 80.5 fb^{-1} of pp 2015-17 data, 13 TeV
- Statistically combined with Run1 ATLAS results:
  - 4.9 fb^{-1} (7 TeV, pp 2011)
  - 14.3 fb^{-1}(8 TeV, pp 2012) - statistically combined with 7 TeV
- Collected by triggers based on identification of J/ψ with pT(μ) threshold (mainly 4 and 6 GeV)
  - Including MC samples for $B_s \rightarrow J/\psi\phi$ and dedicated backgrounds $B_d \rightarrow J/\psi K^*$, $B_d \rightarrow J/\psi K\pi$ and $\Lambda_b \rightarrow J/\psi pK$
- No lifetime cut - signal-background separation done by the fit

Angular analysis

Eur. Phys. J. C 81 (2021) 342

- $B_s \rightarrow J/\psi\phi$ decay=decay of pseudoscalar to vector-vector
- Final state: admixture of CP-odd (L = 1) and CP-even (L = 0, 2) states
- Distinguishable through time-dependent angular analysis
- Non-resonant S-wave decay $B_s \rightarrow J/\psi KK$ contribute to the final state and is included in the differential decay rate due to interference with the $B_s \rightarrow J/\psi(\mu\mu)\phi(KK)$ decay
- The transversity angles, $\Omega = (\Theta_T , \Psi_T , \varphi_T)$ are defined as below

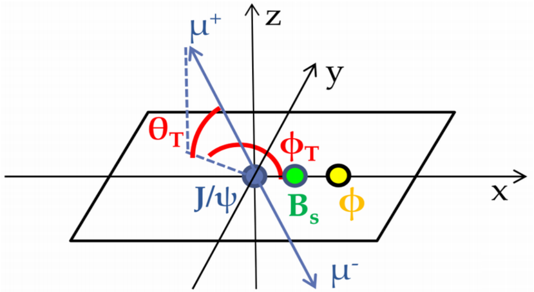

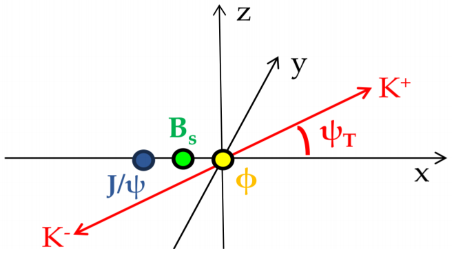

Opposite-side flavour tagging

Eur. Phys. J. C 81 (2021) 342

- Use b-$\bar{b}$ correlation => initial B_s flavour
  - b → l transitions - clean tagging method
  - diluted by oscillations and b → c → l
- Provides probability P(B|Q) of signal candidate to be B_s or $\bar{B}_s$
- Tagger types: tight muon, low-p_T muon, electron, b-tagged jet
- Key variables: charge of p_T-weghted tracks in cone ΔR around the leptons,b-jets

$$Q_x = \frac{\sum_i^{N\ \mathrm{tracks}} q_i \cdot (p_{\mathrm{T}i})^\kappa}{\sum_i^{N\ \mathrm{tracks}} (p_{\mathrm{T}i})^\kappa}$$

- Search order based on best purity: tight muons, electrons, low-p_T muons, b-jets
- Calibrated on self-tagged $B^\pm \to J/\psi K^\pm$ data

$$\mathcal{D}(Q_x) = 2P(B|Q_x) - 1$$
$$T_x = \sum_i \epsilon_{x\,i} \cdot (2P(B|Q_{x\,i}) - 1)^2$$

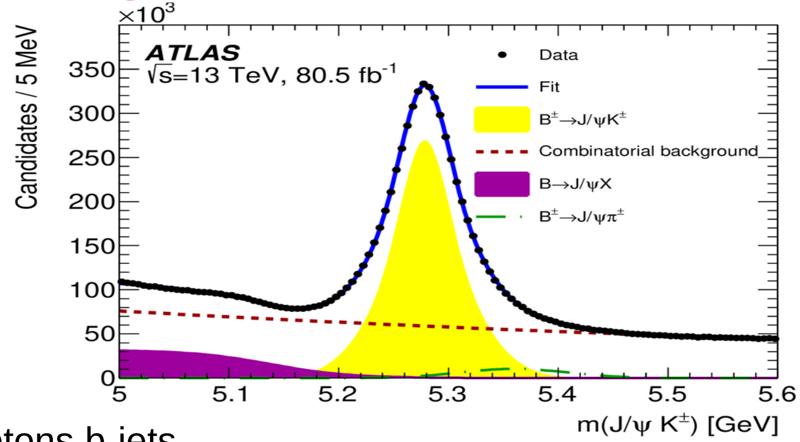

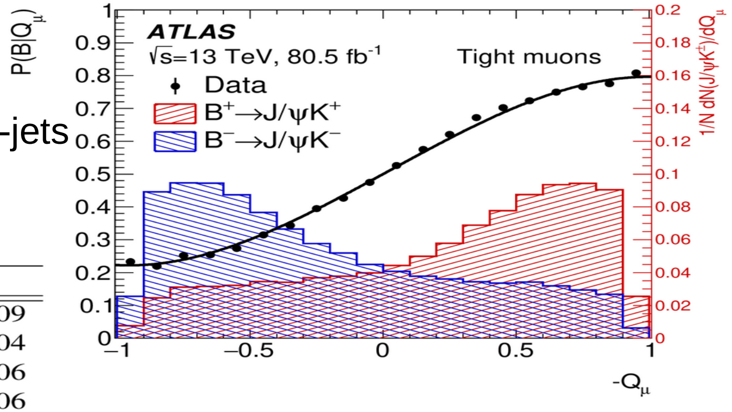

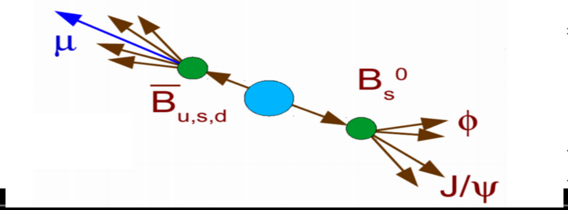

Tag method	ϵ_x [%]	D_x [%]	T_x [%]
Tight muon	4.50 ± 0.01	43.8 ± 0.2	0.862 ± 0.009
Electron	1.57 ± 0.01	41.8 ± 0.2	0.274 ± 0.004
Low-p_T muon	3.12 ± 0.01	29.9 ± 0.2	0.278 ± 0.006
Jet	12.04 ± 0.02	16.6 ± 0.1	0.334 ± 0.006
Total	21.23 ± 0.03	28.7 ± 0.1	1.75 ± 0.01

UML fit and Results

Eur. Phys. J. C 81 (2021) 342

- An unbinned maximum likelihood (UML) fit performed for B_s mass, decay time and the decay angles:

$$\ln\mathscr{L} = \sum_{N}^{i=1} w_i * \ln\left(f_s \mathscr{F}_s + f_s f_{(B^0)} \mathscr{F}_{(B^0)} + f_s f_{(\Lambda_b)} \mathscr{F}_{(\Lambda_b)} + \left(1 - f_s\left(1 + f_{(B^0)} + f_{(\Lambda_b)}\right)\right) \mathscr{F}_{bkg}\right)$$

Observables:

$$\mathscr{F}_x\left(m_i, t_i, \sigma_{m_i}, \sigma_{t_i}, p_{T_i}, \theta_T, \psi_T, \phi_T, P(B|Q_i)\right)$$

Parameter	Value	Statistical uncertainty	Systematic uncertainty
ϕ_s [rad]	−0.081	0.041	0.022
$\Delta\Gamma_s$ [ps^{-1}]	0.0607	0.0047	0.0043
Γ_s [ps^{-1}]	0.6687	0.0015	0.0022
$\lvert A_\parallel(0)\rvert^2$	0.2213	0.0019	0.0023
$\lvert A_0(0)\rvert^2$	0.5131	0.0013	0.0038
$\lvert A_S(0)\rvert^2$	0.0321	0.0033	0.0046
$\delta_\perp - \delta_S$ [rad]	−0.25	0.05	0.04
Solution (a)			
$\delta_\perp$ [rad]	3.12	0.11	0.06
$\delta_\parallel$ [rad]	3.35	0.05	0.09
Solution (b)			
$\delta_\perp$ [rad]	2.91	0.11	0.06
$\delta_\parallel$ [rad]	2.94	0.05	0.09

Two solutions in $\delta_\parallel$ - $\delta_\perp$ plane, with negligible impact on other parameters

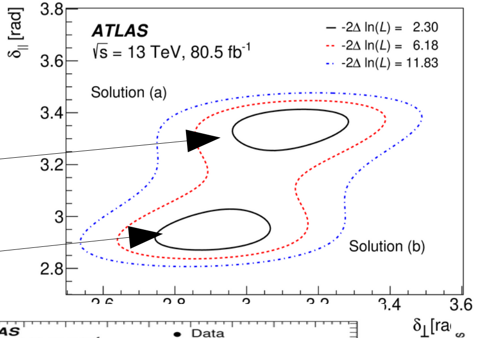

Statistical (BLUE) combination with Run 1 result

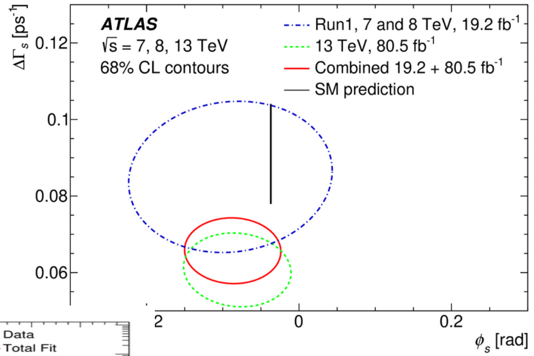

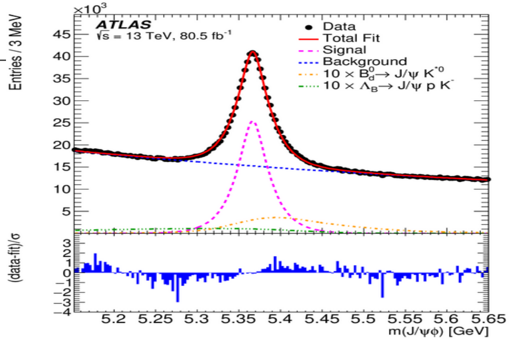

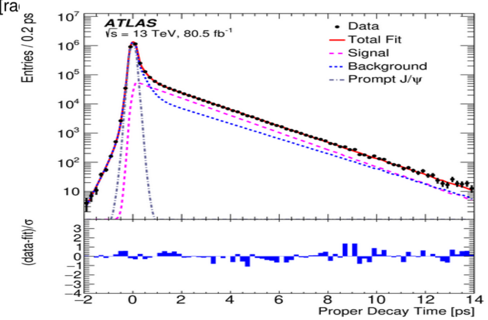

Comparison with other experiments

ATLAS result:

φ_s=−0.087 ± 0.036 (stat.) ± 0.021 (syst.) rad

$\Delta\Gamma_s$=0.0657 ± 0.0043 (stat.) ± 0.0037 (syst.) ps^{-1}

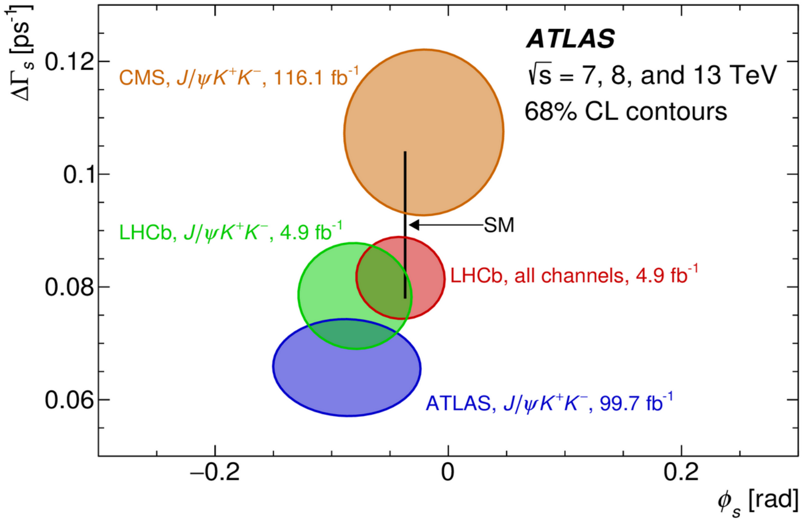

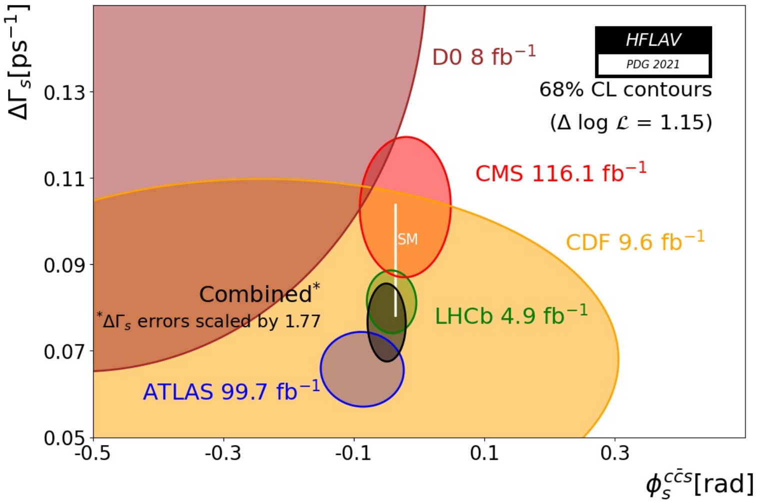

World average:

φ_s= −0.050 ± 0.019 rad

$\Delta\Gamma_s$=0.082 ± 0.005 ps^{-1}

Heavy Flavour Averaging Group (HFLAV 2021)

Study of the rare decays of B_s and B_0 mesons into muon pairs using data collected during 2015 and 2016 with the ATLAS detector

Analysis of rare $B_{(s)} \rightarrow \mu\mu$ decays

JHEP 04 (2019) 098

- Flavour Changing Neutral Currents(FCNC) in the SM proceeding via loop and box diagrams, strongly suppressed ($B \sim 10^{-9}$)
- Beyond SM can signicantly contribute, modifying the branching ratio

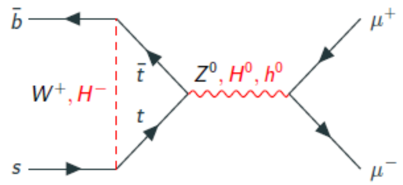

Mesurement(s):

$$B(B_s^0 \rightarrow \mu^+ \mu^-) = N_{d(s)} * \frac{B(B^\pm \rightarrow J/\psi K^\pm) * B(J/\psi \rightarrow \mu^+ \mu^-)}{N_{J/\psi K^\pm} * \frac{\varepsilon_{\mu^+\mu^-}}{\varepsilon_{J/\psi K^\pm}}} * \frac{f_u}{f_{d(s)}}$$

- 36.2 fb^{-1} dataset of 2015-2016 data taking:
  - effectively 26.3 fb^{-1} for $B \rightarrow \mu\mu$
- $B(B_{(s)} \rightarrow \mu\mu)$ mesurement(s) relative to $B(B^\pm \rightarrow J/\psi K^\pm)$, $B_s \rightarrow J/\psi\phi$ as control channel
- Yields $N_{d(s)}$ and $N_{J/\psi K\pm}$ obtained from UML fits to the mass spectra
- Separate signal from background using boosted decision tree (BDT)
- Known branching ratios from PDG, $f_u/f_{d(s)}$ from HFLAV

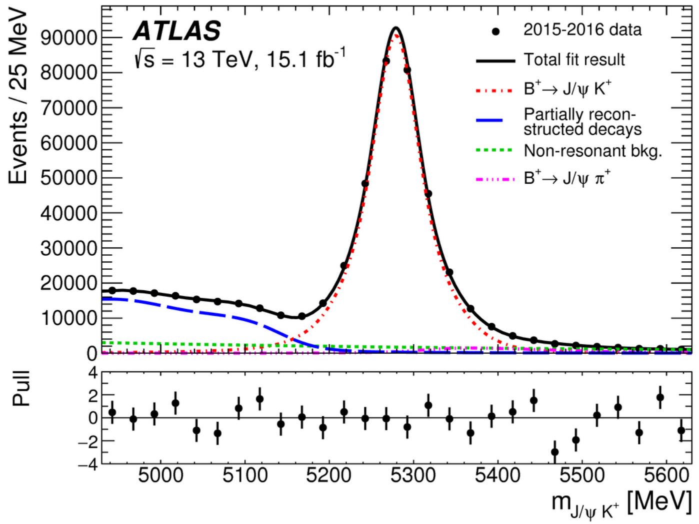

Backgrounds

[JHEP 04 (2019) 098]

Partially reconstructed b-hadron decays

- Mostly in the low di-muon mass region
- Shape parameters is free to be determined in the fit

Peaking backgrounds:

- Hadronic B_s decays where hadrons are misidentified as muons
- Simulated and fixed in the mass fit

Continuum backgrounds:

- Combinatorics of μ and uncorrelated hadron decays
- Reduced by BDT
- Systematics due to $B^\pm_c \to J/\psi\mu\nu$ and $B_{(s)}/\Lambda_b \to h\mu\nu$ decays

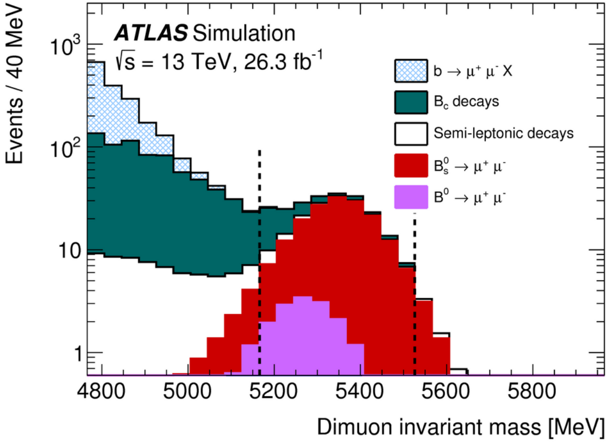

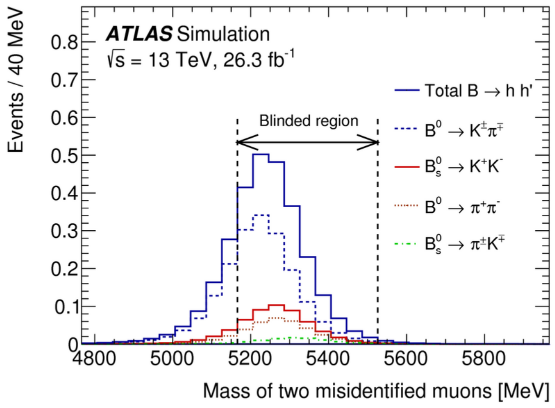

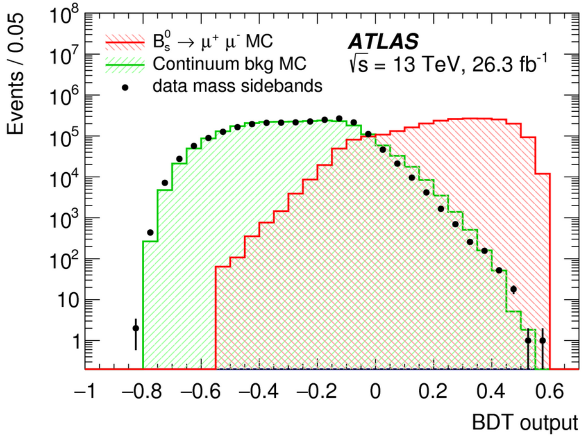

BDT and signal extraction

JHEP 04 (2019) 098

- BDT formed from 15 variables
    - Kinematics, isolation, B-vertex separation from PV
- BDT output validated on reference $B^{\pm} \rightarrow J/\psi K^{\pm}$ and control $B_s \rightarrow J/\psi\phi$ channels observed difference applied as the correction is on the efficiency ratio
- Signal region divided into four BDT bins with constant signal efficiency
- Simultaneous extraction of $B_s \rightarrow \mu\mu$ and $B_d \rightarrow \mu\mu$ yields from UML fit to di-muon mass distributions in the four BDT bins

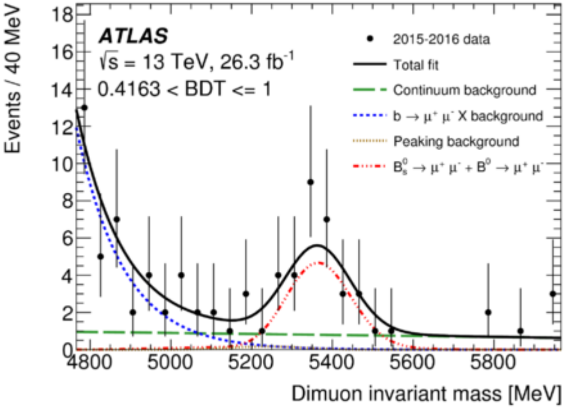

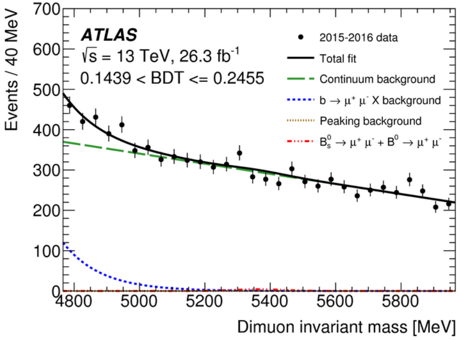

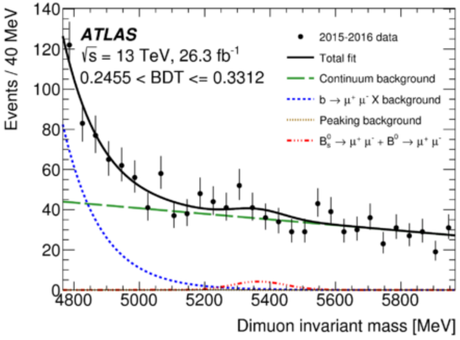

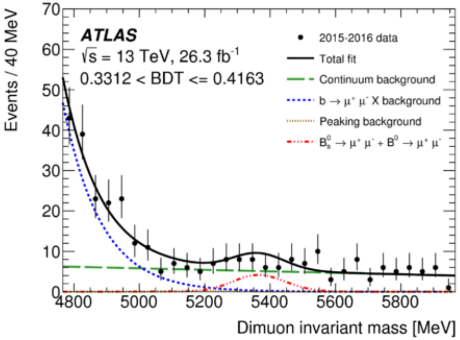

Results

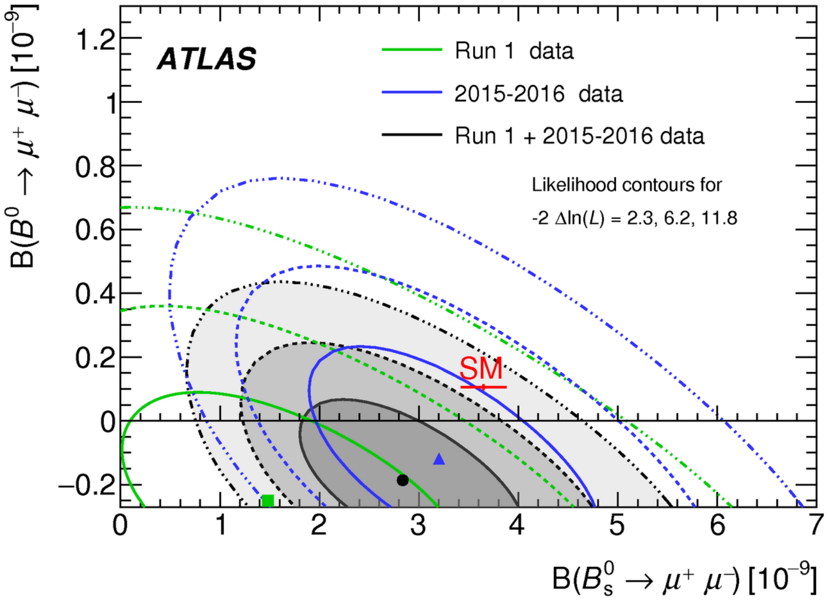

[JHEP 04 (2019) 098]

Standard model:

$$B(B_s^0 \rightarrow \mu\,\mu) = (3.66 \pm 0.14) * 10^{-9}$$
$$B(B_d^0 \rightarrow \mu\,\mu) = (1.03 \pm 0.05) * 10^{-9}$$

arXiv:1908.07011

ATLAS 2015+2016 data:

$$B(B_s^0 \rightarrow \mu\,\mu) = (3.2^{+1.1}_{-1.0}) * 10^{-9}$$
$$B(B_d^0 \rightarrow \mu\,\mu) < 4.3 * 10^{-10}\ at\ 95\%\ CL$$

ATLAS Run1+2015+2016 data:

$$B(B_s^0 \rightarrow \mu\,\mu) = (2.8^{+0.8}_{-0.7}) * 10^{-9}$$
$$B(B_d^0 \rightarrow \mu\,\mu) < 2.1 * 10^{-10}\ at\ 95\%\ CL$$

- Combined measurement compatible with SM at 2.4σ
- Statistic uncertainties dominate

Combination of ATLAS+CMS+LHCb

CMS-PAS-BPH-20-003 ; LHCb-CONF-2020-002 ; ATLAS-CONF-2020-049

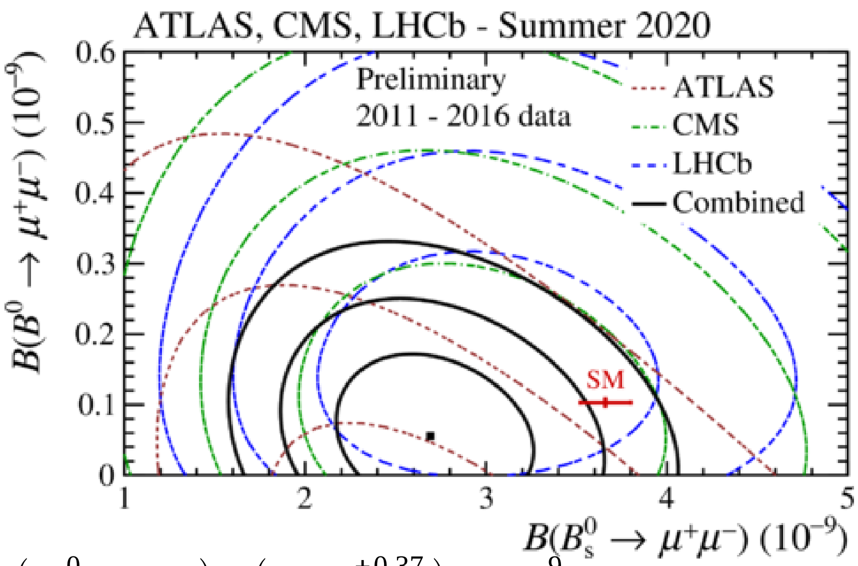

$$B(B_s^0 \to \mu\mu) = (2.69^{+0.37}_{-0.35}) * 10^{-9}$$

$$B(B_d^0 \to \mu\mu) < 1.9 * 10^{-10} \; at\, 95\%\, CL$$

$$Ratio < 0.052 \; at\, 95\%\, CL \, (SM: 0.0281 \pm 0.0016)$$

$$\tau_{B_s^0 \to \mu\mu}[ps](LHCb + CMS) = 1.9^{+0.35}_{-0.37}(SM: 1.609 \pm 0.010)$$

- Combination from binned two-dimensional profile likelihoods
- Independent systematics, except for ratio of fragmentation fractions f_d/f_s, common nuisance parameter and only correlation among experiments
- fd/fs profiled separately and its uncertainty included in a single likelihood
- The results compatible with the SM predictions within 2.1 standard deviations in the 2d plane of the branching fractions

Summary

- Latest ATLAS result measurement of CP-violation in $B_s \to J/\psi\phi$ decay and branching ratio measurement of rare $B_{s(d)} \to \mu\mu$ decays compatible with Standart Model predictions
- Full Run 2 data analyses in progress

Backup

Tagging performance

Tag method	ϵ_x [%]	D_x [%]	T_x [%]
Tight muon	4.50 ± 0.01	43.8 ± 0.2	0.862 ± 0.009
Electron	1.57 ± 0.01	41.8 ± 0.2	0.274 ± 0.004
Low-p_T muon	3.12 ± 0.01	29.9 ± 0.2	0.278 ± 0.006
Jet	12.04 ± 0.02	16.6 ± 0.1	0.334 ± 0.006
Total	21.23 ± 0.03	28.7 ± 0.1	1.75 ± 0.01

- Efficiency: Fraction of signals with specific tagger, $\varepsilon = \frac{N_{tagged}}{N_{Bcand}}$
- Dilution: D = (1 − 2w), where w is the miss-tag probability
- Tagging Power: figure of merit of tagger performance
  - Depends on dilution and efficiency: $TP = \varepsilon D^2 = \varepsilon(1 - 2w)^2$

Reconstruction and candidate selection

Event

- Triggers and good quality data
- At least one PV formed from at least 4 ID tracks
- At least one pair of ID+MS identified $\mu^+\mu^-$

$J/\psi \rightarrow \mu^+\mu^-$

- Dimuon vertex fit χ^2/d.o.f. < 10
- Three dimuon invariant mass windows for BB/BE/EE (barrel,endcap) muon combinations

$\phi \rightarrow K^+K^-$

- $p_T(K) > 1$ GeV
- 1008.5 MeV < m(KK) < 1030.5 MeV

$B_s \rightarrow J/\psi(\mu\mu)\phi(KK)$

- $p_T(B_s) > 10$ GeV
- Four-track vertex fit χ^2/d.o.f. < 3 (J/ψ mass constrained)
- Keep only the candidate with best vertex fit χ^2/d.o.f. in event
- 5150 MeV < $m(B_s)$ < 5650 MeV → in total 3 210 429 B_s candidates

Signal time-angular PDF

k	$O^{(k)}(t)$	$g^{(k)}(\theta_T,\psi_T,\phi_T)$
1	$\frac{1}{2}\lvert A_0(0)\rvert^2\left[(1+\cos\phi_s)\,e^{-\Gamma_L^{(s)}t}+(1-\cos\phi_s)\,e^{-\Gamma_H^{(s)}t}\pm 2e^{-\Gamma_s t}\sin(\Delta m_s t)\sin\phi_s\right]$	$2\cos^2\psi_T(1-\sin^2\theta_T\cos^2\phi_T)$
2	$\frac{1}{2}\lvert A_\parallel(0)\rvert^2\left[(1+\cos\phi_s)\,e^{-\Gamma_L^{(s)}t}+(1-\cos\phi_s)\,e^{-\Gamma_H^{(s)}t}\pm 2e^{-\Gamma_s t}\sin(\Delta m_s t)\sin\phi_s\right]$	$\sin^2\psi_T(1-\sin^2\theta_T\sin^2\phi_T)$
3	$\frac{1}{2}\lvert A_\perp(0)\rvert^2\left[(1-\cos\phi_s)\,e^{-\Gamma_L^{(s)}t}+(1+\cos\phi_s)\,e^{-\Gamma_H^{(s)}t}\mp 2e^{-\Gamma_s t}\sin(\Delta m_s t)\sin\phi_s\right]$	$\sin^2\psi_T\sin^2\theta_T$
4	$\frac{1}{2}\lvert A_0(0)\rvert\lvert A_\parallel(0)\rvert\cos\delta_\parallel\left[(1+\cos\phi_s)\,e^{-\Gamma_L^{(s)}t}+(1-\cos\phi_s)\,e^{-\Gamma_H^{(s)}t}\pm 2e^{-\Gamma_s t}\sin(\Delta m_s t)\sin\phi_s\right]$	$\frac{1}{\sqrt{2}}\sin 2\psi_T\sin^2\theta_T\sin 2\phi_T$
5	$\lvert A_\parallel(0)\rvert\lvert A_\perp(0)\rvert\left[\frac{1}{2}(e^{-\Gamma_L^{(s)}t}-e^{-\Gamma_H^{(s)}t})\cos(\delta_\perp-\delta_\parallel)\sin\phi_s\pm e^{-\Gamma_s t}(\sin(\delta_\perp-\delta_\parallel)\cos(\Delta m_s t)-\cos(\delta_\perp-\delta_\parallel)\cos\phi_s\sin(\Delta m_s t))\right]$	$-\sin^2\psi_T\sin 2\theta_T\sin\phi_T$
6	$\lvert A_0(0)\rvert\lvert A_\perp(0)\rvert\left[\frac{1}{2}(e^{-\Gamma_L^{(s)}t}-e^{-\Gamma_H^{(s)}t})\cos\delta_\perp\sin\phi_s\pm e^{-\Gamma_s t}(\sin\delta_\perp\cos(\Delta m_s t)-\cos\delta_\perp\cos\phi_s\sin(\Delta m_s t))\right]$	$\frac{1}{\sqrt{2}}\sin 2\psi_T\sin 2\theta_T\cos\phi_T$
7	$\frac{1}{2}\lvert A_S(0)\rvert^2\left[(1-\cos\phi_s)\,e^{-\Gamma_L^{(s)}t}+(1+\cos\phi_s)\,e^{-\Gamma_H^{(s)}t}\mp 2e^{-\Gamma_s t}\sin(\Delta m_s t)\sin\phi_s\right]$	$\frac{2}{3}\left(1-\sin^2\theta_T\cos^2\phi_T\right)$
8	$\alpha\lvert A_S(0)\rvert\lvert A_\parallel(0)\rvert\left[\frac{1}{2}(e^{-\Gamma_L^{(s)}t}-e^{-\Gamma_H^{(s)}t})\sin(\delta_\parallel-\delta_S)\sin\phi_s\pm e^{-\Gamma_s t}(\cos(\delta_\parallel-\delta_S)\cos(\Delta m_s t)-\sin(\delta_\parallel-\delta_S)\cos\phi_s\sin(\Delta m_s t))\right]$	$\frac{1}{3}\sqrt{6}\sin\psi_T\sin^2\theta_T\sin 2\phi_T$
9	$\frac{1}{2}\alpha\lvert A_S(0)\rvert\lvert A_\perp(0)\rvert\sin(\delta_\perp-\delta_S)\left[(1-\cos\phi_s)\,e^{-\Gamma_L^{(s)}t}+(1+\cos\phi_s)\,e^{-\Gamma_H^{(s)}t}\mp 2e^{-\Gamma_s t}\sin(\Delta m_s t)\sin\phi_s\right]$	$\frac{1}{3}\sqrt{6}\sin\psi_T\sin 2\theta_T\cos\phi_T$
10	$\alpha\lvert A_0(0)\rvert\lvert A_S(0)\rvert\left[\frac{1}{2}(e^{-\Gamma_H^{(s)}t}-e^{-\Gamma_L^{(s)}t})\sin\delta_S\sin\phi_s\pm e^{-\Gamma_s t}(\cos\delta_S\cos(\Delta m_s t)+\sin\delta_S\cos\phi_s\sin(\Delta m_s t))\right]$	$\frac{4}{3}\sqrt{3}\cos\psi_T\left(1-\sin^2\theta_T\cos^2\phi_T\right)$

Projections on angles

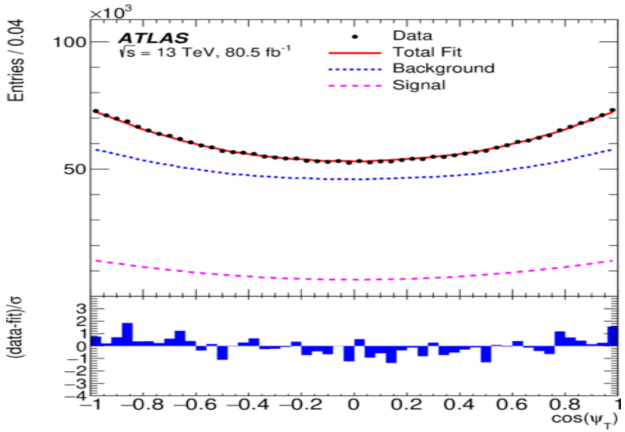

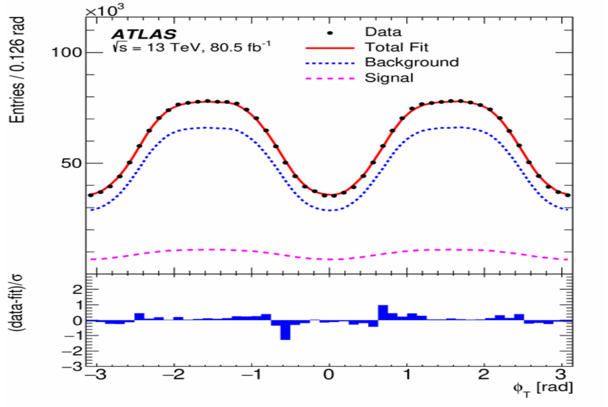

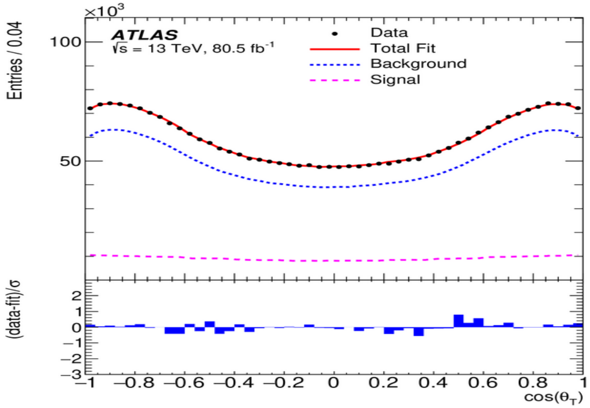

Systematic Uncertainties

arXiv:2001.07115

	ϕ_s [10^{-3} rad]	$\Delta\Gamma_s$ [10^{-3} ps^{-1}]	Γ_s [10^{-3} ps^{-1}]	$\lvert A_\parallel(0)\rvert^2$ [10^{-3}]	$\lvert A_0(0)\rvert^2$ [10^{-3}]	$\lvert A_S(0)\rvert^2$ [10^{-3}]	$\delta_\perp$ [10^{-3} rad]	$\delta_\parallel$ [10^{-3} rad]	$\delta_\perp - \delta_S$ [10^{-3} rad]
Tagging	19	0.4	0.3	0.2	0.2	1.1	17	19	2.3
Acceptance	0.5	< 0.1	< 0.1	1.0	0.8	2.6	30	50	11
ID alignment	0.8	0.2	0.5	< 0.1	< 0.1	< 0.1	11	7.2	< 0.1
Best candidate selection	0.5	0.4	0.7	0.5	0.2	0.2	12	17	7.5
Background angles model:									
Choice of fit function	2.5	< 0.1	0.3	1.1	< 0.1	0.6	12	0.9	1.1
Choice of p_T bins	1.3	0.5	< 0.1	0.4	0.5	1.2	1.5	7.2	1.0
Choice of mass interval	0.4	0.1	0.1	0.3	0.3	1.3	4.4	7.4	2.3
Dedicated backgrounds:									
B_d^0	2.3	1.1	< 0.1	0.2	3.0	1.5	10	23	2.1
Λ_b	1.6	0.3	0.2	0.5	1.2	1.8	14	30	0.8
Fit model:									
Time res. sig frac	1.4	1.1	0.5	0.5	0.6	0.8	12	30	0.4
Time res. p_T bins	0.7	0.5	0.8	0.1	0.1	0.1	2.2	14	0.7
S-wave phase	0.2	< 0.1	< 0.1	0.3	< 0.1	0.3	11	21	8.4
Fit bias	4.1	1.7	0.9	1.4	< 0.1	1.5	19	0.9	7.0
Total	20	2.5	1.6	2.3	3.5	4.5	50	79	18

Uncertainty in the calibration of the B_s-tag probability; MC statistical uncertainty included in fit stat. error

Alternative detector acceptance fit-functions and binning determined from MC

Radial expansion uncertainties determined from their effect on tracks d_0 in the data

Background angles model (fixed in UML fit) extracted from data with varying sidebands size and binning

Uncertainties of relative fraction; fit-model and P-wave contribution

Uncertainties of relative fraction; fit-model and contributions from $\Lambda_b \to J/\psi Kp$ decays

Toy-MC studies; pulls of the default fit model, default fit on toy-data generated with modified PDFs